Quantum Monte Carlo investigation of small ^{4}He clusters with a ^{3}He impurity

Dario Bressanini[a] and Matteo Zavaglia
Dipartimento di Scienze Chimiche, Fisiche e Matematiche, Universitá dell'Insubria, Polo di Como, via Lucini 3, 22100 Como, Italy

Massimo Mella[b] and Gabriele Morosi[c]
Dipartimento di Chimica Fisica ed Elettrochimica, Universitá degli Studi di Milano, via Golgi 19, 20133 Milano, Italy

(Received 27 July 1999; accepted 13 October 1999)

Small helium (^{4}He) clusters containing the lighter isotope ^{3}He are studied by means of quantum Monte Carlo methods. Accurate ground state energies and structural properties are obtained using accurate trial wave functions and the Tang–Tonnies–Yiu (TTY) helium–helium pair potential. The dimer ^{4}He–^{3}He is not bound; as well as the trimer ^{4}He^{3}He$_2$. The smallest cluster containing ^{3}He is ^{4}He$_2$ ^{3}He with a nonrigid structure having a marked linear contribution. Interestingly, this weakly bound system, with an energy one order of magnitude less than the ^{4}He$_3$ trimer, is able to bind another ^{3}He atom, forming the tetramer ^{4}He$_2$ ^{3}He$_2$, which shows the odd feature of having five out of six unbound pairs. In general, the substitution of a single ^{4}He atom in a pure cluster with a ^{3}He atom leads to an energetic destabilization, as the pair ^{4}He–^{3}He is not bound. The isotopic impurity is found to perturb only weakly the distributions of the remaining ^{4}He atoms, which retain the high floppiness already found in the pure clusters. As the number of atoms increases the isotopic impurity has the marked tendency to stay on the surface of the cluster. This behavior is consistent with the formation of the so-called ''Andreev states'' of a single ^{3}He in liquid ^{4}He helium and droplets, where the impurity tends to form single-particle states on the surface of the pure ^{4}He. © *2000 American Institute of Physics.* [S0021-9606(00)30802-9]

I. INTRODUCTION

In recent years weakly bound atomic and molecular clusters have attracted the attention of a growing number of experimentalists and theoreticians. They offer the unique opportunity to study how matter properties change as a function of the number of atomic and molecular species in the cluster, bridging the gap between isolated gas phase species and bulk matter limit.[1] Clusters containing an impurity can be useful to study at the microscopic level the effect of the solvent on the solute. From the experimental side, the availability of techniques for synthesizing clusters of variable size has opened up new directions of research. Clusters of the desired size are now produced by free jet expansion of the corresponding gases. Since the expansion cools the gas below the condensation temperature, by adjusting the pressure it is possible to stop the condensation when the clusters reach the desired size. These clusters can, eventually, pick up an impurity, and then be probed using a variety of spectroscopic techniques. From the theoretical side, the main obstacle to an accurate first-principle study comes from the failure of the harmonic approximation and normal mode analysis. van der Waals clusters are not rigid structures that vibrate around an equilibrium configuration; rather, they show large-amplitude motions, and even the intuitive notion of equilibrium structure becomes ill defined. Recent efforts have been directed towards the development of methods that treat all the coupled internal degrees of freedom and towards the determination of accurate two-body potentials from which one can build an approximate, but hopefully rather accurate, many-body potential. The question of how important are three- and many-body effects in the description of the cluster is still an active field of research.

The combination of the extremely weak interaction between helium atoms and the small atomic mass makes helium clusters very weakly bound and by far the most intriguing van der Waals clusters with highly quantum features.[2–5] The most interesting feature is with no doubt the possibility to attain a superfluid state with a relatively small number of ^{4}He atoms.[6–8] The superfluidity in helium clusters and the low temperature can be fruitfully exploited to perform high-resolution vibrational and rotational spectroscopy on impurities and to study molecular reaction dynamics of chemical reactions. In a recent experiment, for example, the electronic spectra of the aminoacids tryptophan and tyrosine[9] were simplified by cooling their vibrational motion inside an helium droplet, allowing an easier interpretation of the experimental results.

It is also possible to use an atom or a molecule as a probe to study the local environment of the clusters: to this end a great variety of atoms and molecules has been included in the clusters.

The systems formed by the two helium isotopes, even-

[a]Electronic mail: dario@fis.unico.it
[b]Electronic mail: Massimo.Mella@unimi.it
[c]Electronic mail: Gabriele.Morosi@unimi.it

tually doped with an atomic or molecular impurity, are of particular interest. Since the helium–helium interaction potential does not distinguish between the two isotopic species, it is possible to study effects entirely due to the zero-point motion of the species and to the different obeying statistics. A great deal of work has been devoted to the study of ^{4}He/^{3}He liquid mixtures and to the investigation of a single fermionic helium in liquid ^{4}He.[10–13] In the liquid phase, below the tricritical point temperature, increasing the concentration of ^{3}He results in the separation of the mixture in two phases; a ^{4}He- and a ^{3}He-rich phase. For $T\rightarrow 0$ the ^{3}He solubility in ^{4}He reaches a finite value. The ^{3}He atom, being lighter, tends to move in regions of low ^{4}He density. For systems with a free surface, the fermionic atoms have the tendency to move to the surface, where they experience an effective potential and form the so called Andreev states.[14]

With the availability of modern diffraction techniques from a transmission grating, the study of mixed ^{4}He/^{3}He droplets has received a major impetus, both theoretical and experimental.[5,15–19]

Theoretical studies of mixed ^{4}He/^{3}He droplets, using density functional[15] or variational Monte Carlo techniques,[16] predicted the formation of Andreev states on the surface of medium size droplets. They also showed that the binding energy of the ^{3}He surface states approaches the binding energy of ^{3}He atoms on a planar ^{4}He surface, as the number of atoms is increased.

Surprisingly, while there has been a large theoretical effort in the accurate study of pure ^{4}He and ^{3}He small clusters, very little has been done towards the investigation of small mixed $^4\mathrm{He}_N\,^3\mathrm{He}_M$ clusters. With the exception of the studies on the trimers $^4\mathrm{He}_3$, $^4\mathrm{He}_2\,^3$He, and ^{4}He $^3\mathrm{He}_2$,[20–26] results for other small systems are scattered[27,28] and, to our knowledge, there are no accurate investigations using one of the modern helium–helium interaction potentials.

In this work we study the energetics and structure of the ground state of the $^4\mathrm{He}_N\,^3$He clusters using quantum Monte Carlo (QMC) techniques. In the past decade, QMC methods have been invaluable in providing a clear picture of highly quantum clusters of hydrogen and helium, both pure and doped with an impurity.[2–5,29–39] Here we use QMC methods to understand the structure of these systems, by computing various distributions of the two helium isotopes.

The rest of the paper is organized as follows: Sec. II gives a brief description of the theoretical approach and the computational methods used. Section III contains a discussion of our results, while Sec. IV reports our conclusions and possible future directions of this study.

II. COMPUTATIONAL METHODS

It has become clear in the last few years that the only methods able to accurately estimate the properties of highly quantum clusters are the quantum Monte Carlo methods. They have been successfully employed in the past in the study of pure and doped helium clusters and are well described in the literature. For this reason we summarize here only the main points of the methods that are relevant to the discussion of this work, while we redirect the reader to the vast literature on the subject for more technical details and for a review of the applications of these methods.[40–43]

In atomic units, the Hamiltonian operator for the mixed $^4\mathrm{He}_N\,^3\mathrm{He}_M$ cluster is

$$\hat{H}=-\frac{1}{2}\left(\sum_{i=1}^{N}\frac{\nabla^2}{m_4}+\sum_{i=1}^{M}\frac{\nabla^2}{m_3}\right)+V(\mathbf{R}), \tag{1}$$

where $V(\mathbf{R})$ is the interaction potential between the helium atoms and $\mathbf{R}$ is a point in configuration space that represents the position of all the species. For the atomic masses we used $m_4=7296.12$ amu and $m_3=5497.88$ amu. Here we assume a potential of the form,

$$V(\mathbf{R})=\sum_{i<j}V_{\mathrm{He-He}}(r_{ij}), \tag{2}$$

where r_{ij} is the distance between two helium atoms and $V_{\mathrm{He-He}}(r)$ is the two body interaction potential. We explicitly exclude three-body terms which are believed to be unimportant for small helium clusters. We use the recently developed Tang–Tonnies–Yiu potential[44] (TTY) for the pair interaction. This potential, which is not based on any kind of empirical information, has been used recently by Lewerenz[32] in his study of small pure ^{4}He clusters. We chose it in order to more easily check our computer code by comparing our results for pure clusters with those published. This potential is known to give a slightly weaker binding, in comparison with the less recent and more commonly used HFD-B(He) potential,[45] likely owing to the stronger repulsion term. These small differences should not affect the results of this work. Notice that the interaction potential between two helium atoms is the same regardless the masses, so any effect on the energetics and structure of the mixed clusters $^4\mathrm{He}_N\,^3\mathrm{He}_M$, as long as $M<3$, should be ascribed only to the different zero-point motion of the two species. For $M\geqslant 3$ effects due to the different obeying statistics become important.

We approximate the ground state wave function of the cluster $^4\mathrm{He}_N\,^3$He with the pair-product form

$$\Psi_T(R)=\prod_{i<j}^{N}\varphi(r_{ij})\prod_{k}^{N}\phi(r_k), \tag{3}$$

where r_{ij} is the distances between two ^{4}He atoms while r_k is the distance between the ^{3}He impurity and a ^{4}He atom. For the pure cluster we simply omit the impurity product. Both the $\varphi(r)$ and $\phi(r)$ functions have the same analytical form,

$$\varphi(r)=\phi(r)=\exp\left(-\frac{p_5}{r^5}-\frac{p_2}{r^2}-p_0\ln(r)-p_1 r\right), \tag{4}$$

which has been used with success for the description of small helium clusters by several workers.[32,39,46] We found unnecessary to include one-body functions; as a result the trial wave function is translationally invariant and this guarantees that we are not introducing any spurious kinetic energy of the center of mass. The chosen form for the trial wave function makes impossible to compute analytically the matrix element of the Hamiltonian operator, so a numerical method must be used to estimate the variational energy and other properties for a given choice of the eight parameters. An

integration method well suited for high dimensional spaces is the Monte Carlo method. Its practical application to the computation of the variational energy of a given trial wave function is called variational Monte Carlo[40,41,43] (VMC). The VMC approach is a very powerful technique that estimates the energy and all the desired properties of a given trial wave function without any need to compute analytically the matrix elements. For this reason, it poses no restrictions on the functional form of the trial wave function, requiring only the evaluation of the wave function value, its gradient, and its Laplacian, and these are easily computed. Although the VMC approach, with a proper choice of the trial wave function, can give very good results by itself, in this work it has been mainly used to optimize a good trial function to be subsequently employed in a diffusion Monte Carlo (DMC) simulation which is able to estimate the exact ground state energy of the cluster.

All the mean values are computed by using the formula

$$\langle O\rangle = \frac{\int f(\mathbf{R}) O_{\mathrm{loc}}(\mathbf{R}) d\mathbf{R}}{\int f(\mathbf{R}) d\mathbf{R}}, \tag{5}$$

where

$$O_{\mathrm{loc}}(\mathbf{R}) = \frac{O\Psi_T(\mathbf{R})}{\Psi_T(\mathbf{R})} \tag{6}$$

and $f(\mathbf{R})=\Psi_T^2(\mathbf{R})$ for VMC while $f(\mathbf{R})=\Psi_T(\mathbf{R})\Psi_0(\mathbf{R})$ for DMC, $\Psi_0(\mathbf{R})$ being the exact ground state wave function.

The optimization is performed using the standard *fixed sample sigma minimization* algorithm, introduced by Frost[47] and Conroy[48] and recently described by Umrigar, Wilson, and Wilkins.[49] This is the standard way to optimize trial wave functions using VMC. Briefly, the mean square deviation of the local energy $H\Psi/\Psi$ is minimized, rather than the energy itself, since this leads to a numerically more stable process. The fluctuation of the local energy $\sigma^2(H)=\langle H^2\rangle - \langle H\rangle^2$ is computed using an ensemble of points (or *walkers*) distributed in configuration space. After the optimization has produced a new function, a VMC simulation is performed to estimate the new trial energy and to generate a new ensemble of walkers, to be used eventually in a new optimization. Usually convergence is achieved in three or four steps.

III. RESULTS AND DISCUSSION

In order to check our computer code, we have recomputed the energies of pure helium clusters for $N=2-7$ using the wave functions optimized by Rick, Lynch, and Doll[4] and recently used by Lewerenz.[32] The DMC energies are in optimal agreement with those obtained by Lewerenz, our results have a smaller error bar as a result of longer simulations. We also optimized the wave functions for $^4He_{11}$ and $^4He_{20}$ in order to compare these slightly larger pure clusters with those containing an impurity. As to the clusters containing an impurity, their wave functions have been optimized starting from the wave functions of the corresponding pure clusters. A minimum of 5000 configurations has been used during the optimization steps and for the VMC and DMC simulations. A time step of 200 hartree^{-1} has been employed for all the DMC simulations and we checked that the time step bias was within the statistical error of the calculations by performing a few simulations with a smaller time step. The trial wave functions employed in this work are only an approximation to the exact ground state wave functions, and give only approximate estimations of the true properties of these clusters. In order to project out the remaining excited states contributions we used the DMC method to sample the distribution $f(\mathbf{R})=\Psi_T(\mathbf{R})\Psi_0(\mathbf{R})$ which, using Eq. (5), allows the estimation of the exact ground state energy. In the DMC method, the mixed estimator does not give the exact values for operators that do not commute with the Hamiltonian, but only an approximation, albeit more accurate than the VMC estimate. For these properties, namely radial distributions, we give a more correct estimation using the so called ''second order estimation'' (SOE),

$$\langle O\rangle_{\mathrm{SOE}} = 2\langle O\rangle_{\mathrm{DMC}} - \langle O\rangle_{\mathrm{VMC}}. \tag{7}$$

This gives an estimate of $\langle O\rangle$ that is second order on the error of the trial wave function.

TABLE I. DMC and VMC energies (cm^{-1}) for He_N and $^4He_{N-1}$ ^{3}He clusters.

N	DMC ^4He_N	VMC $^4He_{N-1}$ ^{3}He	DMC $^4He_{N-1}$ ^{3}He
2	−0.00089(1)		
3	−0.08784(7)	−0.00666(2)	−0.00984(5)
4	−0.3886(1)	−0.19199(2)	−0.2062(1)
5	−0.9015(3)	−0.57484(6)	−0.6326(2)
6	−1.6077(4)	−1.1505(2)	−1.2626(4)
7	−2.4805(7)	−1.8595(2)	−2.0718(5)
11	−7.286(1)	−5.975(3)	−6.679(4)
20	−23.04(1)	−19.98(1)	−22.234(9)

The energy estimates of the DMC simulations of the pure clusters, and the VMC and DMC results of the mixed clusters are shown in Table I. The differences between the VMC and DMC values are a manifestation of the deficiencies of the trial wave functions and the optimization process. On one hand the trial wave functions were not optimized to give the best energy, but instead to give a low $\sigma(H)$, and we do not know which is the best energy for a given trial wave function. It is well known that the optimization of the energy within a VMC simulation is numerically a very unstable process and so we are forced to optimize the sigma. On the other hand the contributions of three- and many-body terms in the wave functions might be important and the description of the wave function in the repulsive part of the potential should be improved. A major hint that there is a need for a better trial wave function form comes also from the fact that, as already noticed in previous works, it is very difficult to optimize these functions. It was especially hard to optimize the trimers wave function and this might explain why the relative energy recovered on going from VMC to DMC appears to be larger than for the other clusters. Work is under way in our laboratory to develop more accurate, but nevertheless still compact wave functions for helium clusters.

Figure 1 shows that both the total energies for the pure and the doped clusters follow a quadratic relation with very good approximation. This can be rationalized qualitatively for the pure clusters by considering that, in absence of three-

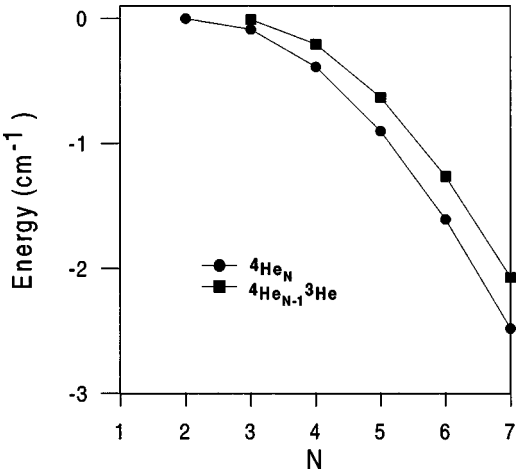

FIG. 1. DMC energies for the ^4He_N and $^4He_{N-1}\,^3He$ clusters, for $N \leqslant 7$.

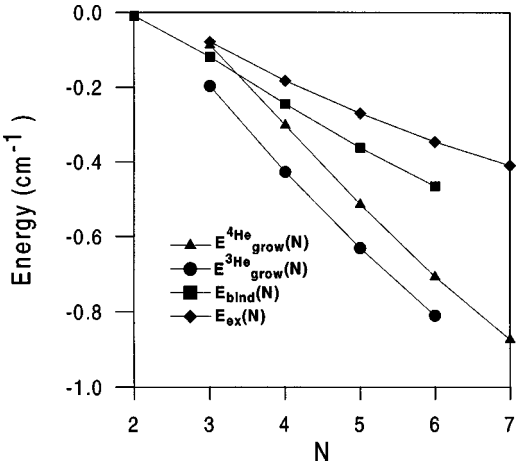

FIG. 2. Energetic quantities defined in Eq. (8).

body terms in the potential, the energy is roughly proportional to the number of pairs present. If in a ^4He_N cluster we substitute a ^4He with a ^3He the energy is perturbed by a factor linear in the number of particles, since now there are $N-1$ ^3He–^4He unbound pairs. As a result, the quadratic character of the energy trend is not changed.

To avoid cluttering the equations too much, we indicate with the symbol $E(N,M)$ the energy of the system $^4He_N\,^3He_M$, where in this work M can be either 0 or 1.

From the total energies, it is possible to define some related quantities that can give more insight into the energetics of these systems,

$$\begin{aligned} E_{\text{bind}}(N) &= E(N,1) - E(N,0), \\ E_{\text{ex}}(N) &= E(N,0) - E(N-1,1), \\ E^{^4\text{He}}_{\text{grow}}(N) &= E(N,0) - E(N-1,0), \\ E^{^3\text{He}}_{\text{grow}}(N) &= E(N,1) - E(N-1,1), \end{aligned} \tag{8}$$

where $E_{\text{bind}}(N)$ represents the binding energy of the impurity ^3He to a pure cluster of ^4He atoms, $E_{\text{ex}}(N)$ represents the energy released by exchanging a boson atom with a fermion atom, and finally $E^{^4\text{He}}_{\text{grow}}(N)$ and $E^{^3\text{He}}_{\text{grow}}(N)$ represents the energy released by adding a ^4He atom to an already formed $^4He_{N-1}$ or $^4He_{N-1}\,^3He$, respectively. Of course, these quantities are not all independent, as for example,

$$\begin{aligned} E^{^3\text{He}}_{\text{grow}}(N) - E_{\text{ex}}(N) &= E_{\text{bind}}(N), \\ E^{^4\text{He}}_{\text{grow}}(N) - E_{\text{ex}}(N) &= E_{\text{bind}}(N-1). \end{aligned} \tag{9}$$

These quantities are shown in Fig. 2. Since the total energies scale quadratically, it is not surprising that both the growth energies follow an almost linear relationship, since the quadratic component due to the ^4He–^4He interactions is subtracted out. For the same reason, the binding energy for these small clusters must follow a linear law.

Previous studies with other small impurities like H^- (Ref. 50) and H_2 (Ref. 29) had shown that the energies of those systems are dominated by the presence of the impurity. This is unlike what we have found here and the reason is again to be ascribed to the lack of bonding between the two helium isotopes.

The hypothetical dimers $^4He^3He$ and $^3He^3He$ are not known and are believed to be unbound, so is not completely surprising that the trimer $^4He^3He_2$ is unstable (although the possibility of borromean binding[51] could not be excluded *a priori*). In fact we have not been able to find a stable ground state for this system, and the DMC simulations showed all the constituent particles to go away from each other. This confirms the findings of other previous works.[22,23,28] The trimer $^4He_2\,^3He$ instead is a stable entity, albeit very weakly bound. Its total energy is one order of magnitude smaller than the pure trimer $^4He_3$. Nevertheless it is possible to add a second ^3He atom and form the stable species $^4He_2\,^3He_2$. We were able to optimize a trial wave function with a VMC energy of $-0.0595(1)$ cm^{-1} and a DMC energy of $-0.071(1)$ cm^{-1}. This tetramer has the odd feature of having five out of six unbound pairs. Notice also that it has a total energy smaller than the $^4He_3$ trimer. Work is underway in our laboratory to characterize the structural properties of this weakly bound tetramer.

During the simulations, many distribution functions were gathered in order to gain insight on the structural properties of these systems. In particular the radial distributions $R(r)$ of the two isotopic species with respect to the center of mass,

$$\mathbf{R}_{\text{CM}} = \frac{m_4 \Sigma_i^{^4\text{He atoms}} \mathbf{r}_i + m_3 \mathbf{r}_{^3\text{He}}}{\Sigma_i^{^4\text{He atoms}} m_4 + m_3} \tag{10}$$

have been gathered during the VMC and DMC simulations. From these, a second order estimation of the exact radial distribution functions has been obtained. We found the SOE radial distribution functions almost identical to those computed with DMC for the smallest clusters, but slightly different for the biggest clusters.

The distributions obtained for the ^4He component, shown in Fig. 3, are very similar to those obtained by Lewerenz[32] showing that the fermionic impurity does not destroy the structure of the remaining bosonic atoms. In fact the radial distribution of ^3He with respect to the geometric

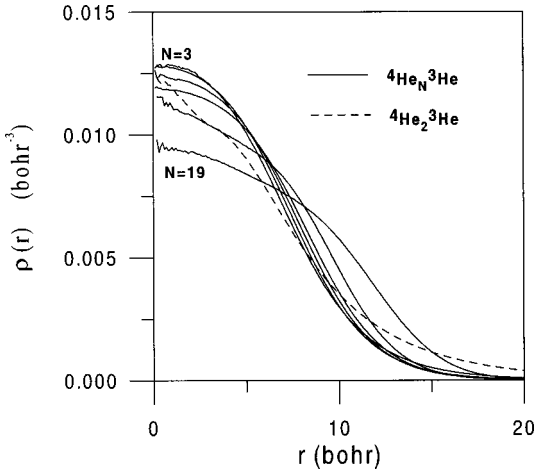

FIG. 3. ^4He distribution with respect the center of mass in the $^4He_N\,^3He$ clusters reported in Table I. The density for $r=0$ decreases monotonically on going from $N=3$ to $N=19$. The distribution of the trimer $^4He_2\,^3He$, which behaves differently, is indicated with the dashed line.

center shows (see Fig. 4) that the fermionic atom is pushed far away from the center of the cluster, as the number of atoms increases. A feature in the distribution of the cluster $^4He_3$ already noticed several times in the past is the local maximum for $r\to 0$. It was interpreted as a tendency of the trimer to be in a linear configuration. The same tendency is present in the $^4He_2\,^3He$ trimer distribution, where the fermionic helium has a finite probability to be found in the center of mass of the two other atoms. For $r\to\infty$ the tail of the distribution decays more slowly than the other distributions, showing the more diffuse nature of the trimer.

As the number of ^4He atoms increases, the density of ^3He at $r=0$ decreases, while the maximum of the distribution moves to larger values. Even for such a small number of atoms, it is already apparent the tendency of the ^3He atom to move to the surface of the system where, for large N, it will form Andreev states.[14]

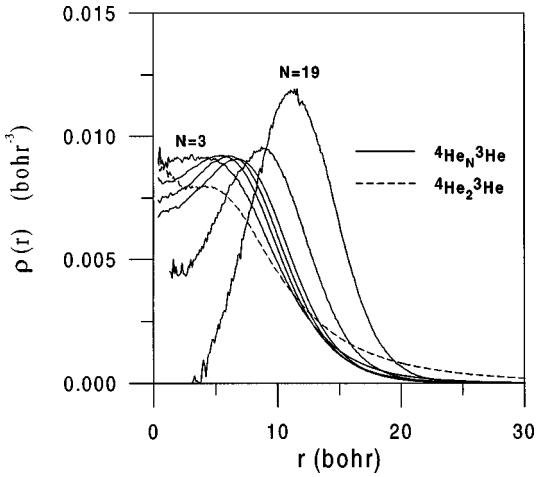

FIG. 4. ^3He distribution with respect the center of mass in the $^4He_N\,^3He$ clusters reported in Table I. The maximum of the distribution moves to larger r on going from $N=3$ to $N=19$. The distribution of the trimer $^4He_2\,^3He$, which shows a marked local maximum for $r=0$, is indicated with a dashed line.

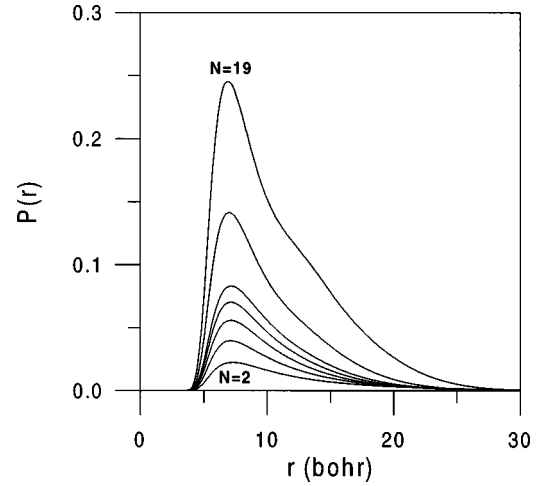

FIG. 5. $^4He-^4He$ pair function in the $^4He_N\,^3He$ clusters reported in Table I.

The pair distribution functions $P(r)$ of $^4He-^4He$ and $^4He-^3He$ are shown in Figs. 5 and 6, respectively. These distributions are normalized such that $\int_0^\infty P(r)r^2dr=S$, where S is the number of atoms of a given species. Again, the distributions for the trimer are somewhat different than the other curves, due to the peculiar characteristics of this cluster. Upon increasing N the maximum of the distributions does not change, as already noticed in the pure clusters. For $N=19$ Figs. 5 and 6 clearly show a marked shoulder in the distribution, a sign of a appearance of a second nearest-neighbor coordination shell. It is interesting to notice that the pair functions between ^3He and ^4He are slightly broader than those between ^4He and ^4He. This is due to the larger zero point motion of the fermionic impurity. For the same reason in the largest clusters the shoulder of the fermionic distribution is more marked and diffused than that of the ^4He atoms.

IV. CONCLUSIONS

In this work we studied the small clusters $^4He_N\,^3He$ by means of quantum Monte Carlo methods obtaining accurate

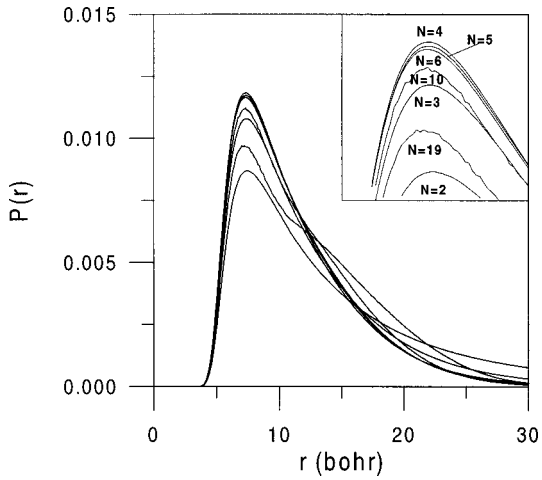

FIG. 6. $^4He-^3He$ pair function in the $^4He_N\,^3He$ clusters reported in Table I. The inset shows the details around the maxima. The value of the maximum increases from $N=2$ to $N=4$ and then decreases. The tail of the trimer distribution falls off less rapidly than the other systems.

ground state energies and structural information. The substitution of a single ^{4}He atom in a pure cluster with a ^{3}He atom leads to an energetic destabilization, due to the presence of the unbound ^{4}He–^{3}He pairs. The isotopic impurity is found to weakly perturb the distributions of the remaining ^{4}He atoms, which retain the high floppiness already found in the pure clusters. The simulations show that the isotopic impurity has the tendency to move on the surface of the cluster. This behavior is consistent with the formation of the so-called ''Andreev states'' of a single ^{3}He in liquid ^{4}He helium and droplets, where the impurity tends to form single-particle states on the surface of the pure ^{4}He.

We confirm that the trimer $^4He^3He_2$ is not bound, while the fragile $^4He_2$ dimer is able to attract a ^{3}He atom and form a trimer. As already found for the pure clusters, this trimer is somewhat different than the other clusters, and it can also be found in a linear configuration.

This weakly bound trimer is able to bind an additional ^{3}He. Although there are two fermionic atoms, the ground state wave function is positive since the two fermions form a singlet state. The addition of a third ^{3}He introduces a node in the ground state wave function and we plan to determine the minimum number of ^{4}He atoms able to bind three ^{3}He atoms in a future work.

[1] Z. Bacic and R. E. Miller, J. Phys. Chem. **100**, 12945 (1996).
[2] R. N. Barnett and K. B. Whaley, Phys. Rev. A **47**, 4082 (1993).
[3] S. A. Chin and E. Krotscheck, Phys. Rev. B **52**, 10405 (1995).
[4] S. W. Rick, D. L. Lynch, and J. D. Doll, J. Chem. Phys. **95**, 3506 (1991).
[5] V. R. Pandharipande, S. C. Pieper, and R. B. Wiringa, Phys. Rev. B **34**, 4571 (1986).
[6] S. Grebenev, J. P. Toennies, and A. F. Vilesov, Science **279**, 2083 (1998).
[7] P. Sindzingre, M. L. Klein, and D. M. Ceperley, Phys. Rev. Lett. **63**, 1601 (1989).
[8] M. V. Rama Krishna and K. B. Whaley, Phys. Rev. Lett. **64**, 1126 (1990).
[9] A. Lindinger, J. P. Toennies, and A. F. Vilesov, J. Chem. Phys. **110**, 1429 (1999).
[10] M. Boninsegni and D. M. Ceperley, Phys. Rev. Lett. **74**, 2288 (1995).
[11] J. Boronat and J. Casulleras, Phys. Rev. B **59**, 8844 (1999).
[12] S. Moroni and M. Boninsegni, Europhys. Lett. **40**, 287 (1997).
[13] F. Pederiva, F. Dalfovo, S. Fantoni, L. Reatto, and S. Stringari, Phys. Rev. B **55**, 3122 (1997).
[14] A. F. Andreev, Sov. Phys. JETP **23**, 939 (1966).
[15] M. Barranco, M. Pi, S. M. Gatica, E. S. Hernandez, and J. Navarro, Phys. Rev. B **56**, 8997 (1997).
[16] A. Belic, F. Dalfovo, S. Fantoni, and S. Stringari, Phys. Rev. B **49**, 15253 (1994).
[17] F. Garcias, L. Serra, M. Casas, and M. Barranco, J. Chem. Phys. **108**, 9102 (1998).
[18] V. R. Pandharipande, J. G. Zabolitzky, S. C. Pieper, R. B. Wiringa, and U. Helmbrecht, Phys. Rev. Lett. **50**, 1676 (1983).
[19] M. Pi, R. Mayol, and M. Barranco, Phys. Rev. Lett. **82**, 3093 (1999).
[20] T. Gonzalez-Lezana, J. Rubayo-Soneira, S. Miret-Artes, F. A. Gianturco, G. Delgado-Barrio, and P. Villarreal, J. Chem. Phys. **110**, 9000 (1999).
[21] T. Gonzalez-Lezana, J. Rubayo-Soneira, S. Miret-Artes, F. A. Gianturco, G. Delgado-Barrio, and P. Villarreal, Phys. Rev. Lett. **82**, 1648 (1999).
[22] E. Nielsen, D. V. Fedorov, and A. S. Jensen, J. Phys. B **31**, 4085 (1998).
[23] B. D. Esry, C. D. Lin, and C. H. Greene, Phys. Rev. A **54**, 394 (1996).
[24] T. Cornelius and W. Glockle, J. Chem. Phys. **85**, 3906 (1986).
[25] S. Huber, Phys. Rev. A **31**, 3981 (1985).
[26] H. S. Huber and T. K. Lim, J. Chem. Phys. **68**, 1006 (1978).
[27] M. Harada, S. Nakaichi-Maeda, T. K. Lim, Y. Akaishi, and H. Tanaka, J. Chem. Phys. **78**, 2102 (1983).
[28] S. Nakaichi, T. K. Lim, Y. Akaishi, and H. Tanaka, J. Chem. Phys. **71**, 4430 (1979).
[29] R. N. Barnett and K. B. Whaley, J. Chem. Phys. **96**, 2953 (1992).
[30] R. N. Barnett and K. B. Whaley, Z. Phys. D: At., Mol. Clusters **31**, 1 (1994).
[31] R. N. Barnett and K. B. Whaley, J. Chem. Phys. **99**, 9730 (1993).
[32] M. Lewerenz, J. Chem. Phys. **106**, 4596 (1997).
[33] M. A. McMahon, R. N. Barnett, and K. B. Whaley, J. Chem. Phys. **99**, 8816 (1993).
[34] M. A. McMahon and K. B. Whaley, Chem. Phys. **182**, 2 (1994).
[35] M. A. McMahon, R. N. Barnett, and K. B. Whaley, Z. Phys. B: Condens. Matter **98**, 421 (1995).
[36] M. A. McMahon and K. B. Whaley, J. Chem. Phys. **103**, 2561 (1995).
[37] M. A. McMahon, R. N. Barnett, and K. B. Whaley, J. Chem. Phys. **104**, 5080 (1996).
[38] M. V. Rama Krishna and K. B. Whaley, Z. Phys. D: At., Mol. Clusters **20**, 1 (1991).
[39] S. W. Rick and J. D. Doll, Chem. Phys. Lett. **188**, 1 (1992).
[40] D. Bressanini and P. J. Reynolds, in *Monte Carlo Methods in Chemical Physics*, edited by D. M. Ferguson, J. I. Siepman, and D. G. Truhlar (Wiley, New York, 1999), Vol. 105, p. 37.
[41] B. Hammond, P. Reynolds, and W. A. Lester, Jr., *Monte Carlo Methods in Ab Initio Quantum Chemistry* (World Scientific, Singapore, 1995).
[42] M. H. Kalos and P. A. Whitlock, *Monte Carlo Methods* (Wiley, New York, 1986).
[43] D. M. Ceperley, G. V. Chester, and M. H. Kalos, Phys. Rev. B **16**, 3081 (1977).
[44] K. T. Tang, J. P. Toennies, and C. L. Yiu, Phys. Rev. Lett. **74**, 1546 (1995).
[45] R. A. Aziz, F. R. McCourt, and C. C. K. Wong, Mol. Phys. **61**, 1487 (1987).
[46] K. B. Whaley, Int. Rev. Phys. Chem. **13**, 41 (1994).
[47] A. A. Frost, J. Chem. Phys. **10**, 242 (1942).
[48] H. Conroy, J. Chem. Phys. **47**, 912 (1967).
[49] C. J. Umrigar, K. G. Wilson, and J. W. Wilkins, Phys. Rev. Lett. **60**, 1719 (1988).
[50] M. Casalegno, M. Mella, G. Morosi, and D. Bressanini, J. Chem. Phys. **112**, 69 (2000).
[51] J. Goy, J.-M. Richard, and S. Fleck, Phys. Rev. A **52**, 3511 (1995).